Inorganic Chemistry

pubs.acs.org/IC

Article

Electrocatalytic Reduction of Nitrogen Oxyanions with a Redox-Active Cobalt Macrocycle Complex

Sheyda Partovi, Ziqing Xiong, Krista M. Kulesa, and Jeremy M. Smith*

Cite This: *Inorg. Chem.* 2022, 61, 9034–9039

Read Online

ACCESS | Metrics & More | Article Recommendations | Supporting Information

ABSTRACT: The cobalt complex, $[Co(CR)Br_2]^+$, where CR is the redox-active macrocycle 2,12-dimethyl-3,7,11,17-tetraazabicyclo-[11.3.1]-heptadeca-1(17),2,11,13,15-pentaene, has been investigated for the electrocatalytic reduction of aqueous NO_2^- and NO_3^-. At neutral pH, the bromide ligands are hydrolyzed, providing $[Co(CR)(OH_2)(OH)]^{2+}$ as the major species in aqueous solution. In the presence of nitrite, $[Co(CR)(NO_2)_2]^+$ is formed as the major species in solution and is a precursor to the electrocatalytic reduction of NO_2^-, which is selectively converted to ammonium with high Faradaic efficiency. There is evidence for both homogeneous and heterogeneous electrocatalysis. Although similar NO_3^- binding is not observed, electrocatalytic reduction to ammonium also occurs, albeit with a lower Faradaic efficiency. In this case, NO_2^- is generated as an intermediate product of NO_3^- reduction.

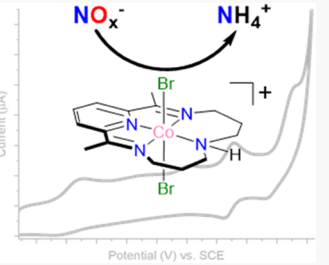

INTRODUCTION

The large-scale accumulation of nitrogen oxyanions (NO_x^-) in the environment is a consequence of the Haber–Bosch process, which generates huge quantities of ammonia from atmospheric nitrogen.[1] While Haber–Bosch ammonia fertilizer is critical to supporting the growing population, of the 135 million tons of agricultural nitrogen that is introduced into the ecosystem, only 17% is consumed as protein.[2] Microbes convert much of the ammonia that is not absorbed by plants to NO_x^-, most notably nitrates (NO_3^-) and nitrites (NO_2^-).[3] Environmental accumulation of water-soluble NO_x^- spurs eutrophication with the resulting algal blooms leading to hypoxic regions.[4,5] In addition, the ingested NO_x^- can lead to serious health complications such as ovarian and bladder cancers, as well as non-Hodgkin's lymphoma.[6]

Electrochemical NO_x^- reduction represents a possible strategy for converting anthropological NO_x^- to benign or useful compounds. Since NO_x^- reduction is a multielectron, multiproton process (e.g., NO_3^- to NH_3 requires eight electrons and nine protons), electrocatalysis is a promising tool for efficient conversion. Molecular electrocatalysts are particularly attractive in this regard since their redox properties can be modified through ligand design, allowing for tunable electrochemistry, control over reactant and product selectivities, and the opportunity for detailed mechanistic insight.[7]

Many homogeneous complexes have been shown to electrocatalytically reduce aqueous NO_3^- or NO_2^- to lower oxidation state compounds such as NH_2OH and NH_3. For example, *trans*-$[Cr(cyclam)Cl_2]^+$ reduces NO_3^- to NO_2^-, although activity is only observed at a mercury pool working electrode.[8,9] By contrast, [Co(2-TMPyP)] (2-TMPyP = tetrakis(N-methyl-2-pyridyl)porphine) reduces NO_2^- to NH_3 and NH_2OH but only in acidic media,[10] while the macrocyclic $[Fe(N_5H_2)Cl_2]^+$ catalyst efficiently reduces NO_2^- to NH_2OH.[11] While these examples hint at a flexibility in design strategies, the structural diversity of these catalysts makes it difficult to elucidate features that are beneficial for NO_x^- reduction.

Focusing on structurally related complexes, particularly those that feature the same metal center, is expected to provide insight into the design features required for the electrocatalytic reduction of aqueous NO_x^-. For example, $[Co(cyclam)Cl_2]^+$ reduces basic NO_3^- and NO_2^- to NH_3 and NH_2OH,[12] while *trans*-$[Co(DIM)Br_2]^+$ (DIM = 2,3-dimethyl-1,4,8,11-tetraazacyclotetradeca-1,3-diene) selectively reduces both NO_3^- and NO_2^- to NH_3 only (Figure 1).[13,14]

The catalytic activity of these cobalt complexes can be related to the properties provided by the supporting macrocycle. Both catalysts are supported by a flexible macrocycle,

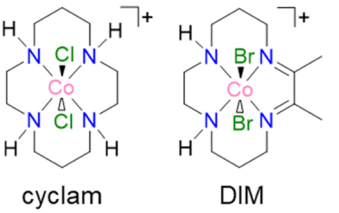

Figure 1. Cobalt macrocycle complexes for electrocatalytic NO_x^- reduction.

Received: January 19, 2022
Published: June 6, 2022

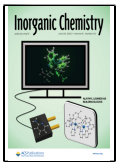

https://doi.org/10.1021/acs.inorgchem.2c00199
Inorg. Chem. 2022, 61, 9034–9039

which can modify its binding mode to accommodate for NO_3^- and NO_2^- as either mono- or bidentate ligands. The redox noninnocence of the DIM ligand allows reducing equivalents to be stored throughout these complexes, in contrast to the redox innocent cyclam ligand. Indeed, $[Co(DIM)Br_2]^+$ reduces NO_3^- at −0.90 V_{SCE}, whereas $[Co(cyclam)Br_2]^+$ has an onset potential of −1.30 V_{SCE}.[15]

Together, these studies suggest a list of ligand design criteria for a molecular electrocatalyst that is active toward NO_3^- and NO_2^- reduction. As exemplified by $[Co(DIM)Br_2]^+$ (Figure 2),[13,14] a macrocycle that provides a combination of redox

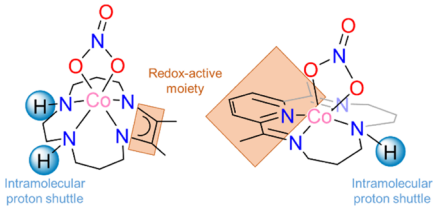

Figure 2. Comparing $[Co(DIM)]^{3+}$ (left) to $[Co(CR)]^{3+}$ (right). $[Co(DIM)]^{3+}$ is known to exhibit both of the criteria above and $[Co(CR)]^{3+}$ is hypothesized to possess the same criteria.

noninnocent character, possible proton shuttles, and flexibility is likely to create a metal complex that is catalytically active toward NO_x^- reduction.

Based on these criteria, we identified the previously reported complex, $[Co(CR)Br_2]^+$,[16] as possessing the necessary attributes for the electrocatalytic reduction of nitrogen oxyanions. The pyridinediimine moiety of the tetraaza macrocycle provides redox noninnocent functionality (Figure 2, orange box),[17] the secondary amine donor provides an intramolecular proton shuttle (Figure 2, blue spheres),[15] and the macrocycle is sufficiently flexible to allow for mono- or bidentate binding of NO_x^- to cobalt.[18−20] In this work, we report on the ability of $[Co(CR)Br_2]^+$ to facilitate the electrocatalytic reduction of both NO_2^- and NO_3^-.

RESULTS AND DISCUSSION

Aqueous Speciation. While $[Co(CR)Br_2]^+$ is olive green in the solid state, its aqueous solutions rapidly become yellow, consistent with the previously reported bromide ligand hydrolysis.[21,22] The ^1H NMR spectrum of $[Co(CR)Br_2]^+$ supports this hypothesis, with resonances for more than one complex observed in D_2O (Figure S3). For example, two sets of pyridyl ring protons are observed, one of which is similar to that previously reported for $[Co(CR)(H_2O)_2](ClO_4)_3$.[23]

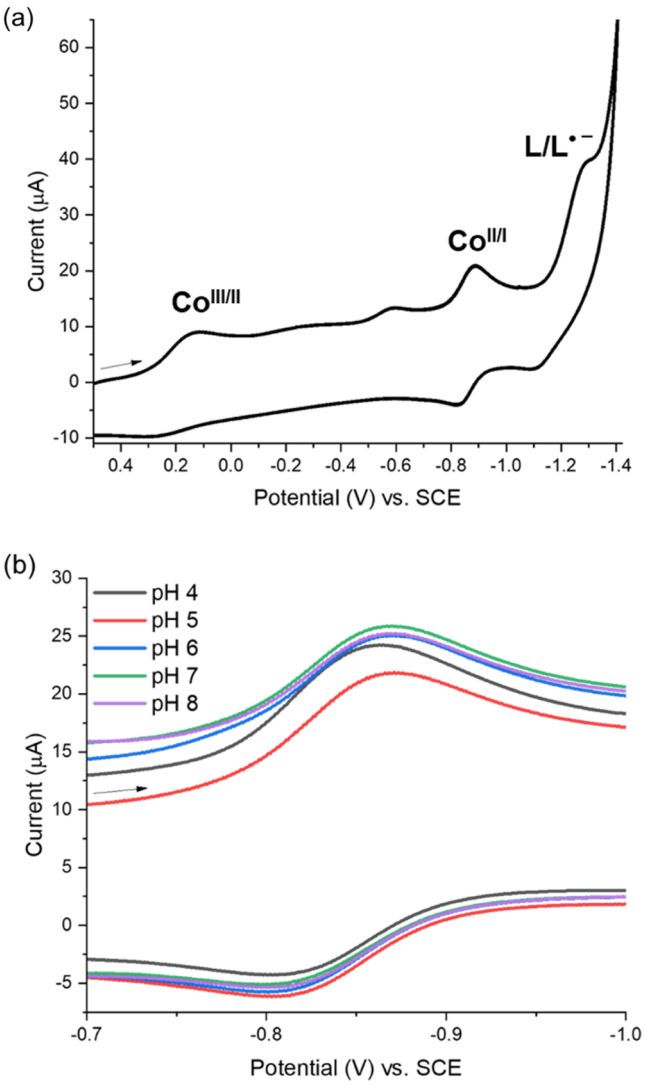

Figure 3. Cyclic voltammograms of 1 mM $[Co(CR)Br_2]^+$ (a) at 0.1 M Na_2SO_4 aqueous solution. The small current at −0.63 V_{SCE} is attributed to catalyst adsorption; (b) 0.1 M Na_2SO_4 aqueous solution with varying pH values. Conditions: glassy carbon working electrode, Pt wire counter electrode, 100 mV s^{-1}.

Aqueous solutions of $[Co(CR)Br_2]^+$ are acidic (e.g., pH 3.32 for a 2.5 mM solution), consistent with the ionization of the aqua ligands. Acid−base titration reveals two ionization events (Figure S5)

$$[Co(CR)(H_2O)_2]^{3+} + H_2O \rightleftarrows [Co(CR)(H_2O)(OH)]^{2+} + H_3O^+,\ pK_a = 4.01$$

$$[Co(CR)(H_2O)(OH)]^{2+} + H_2O \rightleftarrows [Co(CR)(OH)_2]^+ + H_3O^+,\ pK_a = 6.98$$

Together, these results suggest that $[Co(CR)Br_2]^+$ dissolves to provide two compounds in aqueous solution, namely, $[Co(CR)(OH)_2]^{2+}$ and $[Co(CR)(H_2O)(OH)]^{2+}$. Similar aqueous speciation has been observed for $[Co(DIM)Br_2]^+$.[13]

Aqueous Electrochemistry. As previously reported,[21,24,25] three processes are observed in the cyclic voltammogram of $[Co(CR)Br_2]^+$ in acetonitrile solution (Figure S6). We similarly observe three processes in the aqueous-phase cyclic voltammogram of this complex (pH 7; 0.1 M Na_2SO_4). On the basis of their assignments in organic media, these are attributed to a quasi-reversible $Co^{III/II}$ couple (E_{pc} = 0.13 V_{SCE}, E_{pa} = 0.28 V_{SCE}), a reversible $Co^{II/I}$ couple ($E_{1/2}$ = −0.85 V_{SCE}), and an irreversible ligand-based reduction $Co^I(L/L^{\bullet-})$ (E_{pc} = −1.29 V_{SCE}) (Figure 3a).

The $Co^{III/II}$ couple exhibits complex pH-dependent behavior, which is attributed in part to the pH-dependent speciation of the axial ligands, as discussed above (Figures S5 and S8). Similar observations were made for $[Co(CR)Br_2]^+$ in

https://doi.org/10.1021/acs.inorgchem.2c00199
Inorg. Chem. 2022, 61, 9034−9039

organic media.[24] By contrast, the peak potential and current of the $Co^{II/I}$ couple are pH-independent (Figure 3b), suggesting that there is no change in the metal coordination environment on the reduction to Co^{I}. Based on previous work, including single-crystal X-ray diffraction of the lower oxidation states,[24] we suggest that two single-electron reductions of $[Co(CR)Br_2]^+$ provide the five-coordinate Co^{I} complex, $[Co(CR)(OH)]$, in aqueous solution.

Electrochemistry in the Presence of Nitrite. The ^1H NMR spectral changes observed on the addition of excess NO_2^- to an aqueous solution $[Co(CR)Br_2]^+$ suggest that nitrite binds to the metal (Figure S10). Consistent with this, in the presence of 25 mM $NaNO_2$, the quasi-reversible $Co^{III/II}$ couple at 0.13 V_{SCE} shifts cathodically ($E_{pc} = -0.16$ V_{SCE}) from the potential observed in its absence. A similar shift in $Co^{III/II}$ potential was observed for $[Co(DIM)Br_2]^+$ in the presence of NO_2^-.[14] Further titration of NO_2^- leads to additional cathodic shifts in this couple (Figure 4a). In addition, increasing NO_2^- concentration is associated with the onset of electrochemical reversibility. The dependence of $E_{1/2}$ on the NO_2^- concentration can be described according to the Nernst equation (eq 1)[14,26]

$$\Delta E_{1/2} = \frac{RT}{nF} \ln([NO_2^-]) \quad (1)$$

A plot of $E_{1/2}$ *vs.* $\log [NO_2^-]$ yields a linear relationship with a slope of −101 mV/$\log [NO_2^-]$ (Figure S12), suggesting that reduction is coupled to the loss of two NO_2^- ligands, affording the species $[Co(CR)]^{2+}$, which is likely solvent-coordinated

$$[Co(CR)(NO_2)_2]^+ + e^- \rightleftarrows [Co(CR)]^{2+} + 2NO_2^-$$

Cyclic voltammetry reveals that the $Co^{II/I}$ couple is also dependent on NO_2^- concentration, with increasing $[NO_2^-]$ resulting in a loss of reversibility, as illustrated by the anodic shift in the reductive process that is coupled to a disappearance of the oxidative process (Figure 4b). This behavior is characteristic of an EC or ECE process[27] (Figure S12). At the same time, a new oxidative process ($E_{pc} = -0.59$ V_{SCE} at 100 mV/s) is observed with increasing $[NO_2^-]$. The potential of this wave is independent of pH (Figure S13). The scan rate dependence of this new wave is consistent with a freely diffusing species. It is notable that the CV of independently prepared $[Co(CR)NO(Br)]^+$[30] also reveals an oxidative process with $E_{pa} = -0.55$ V_{SCE} at 100 mV/s (Figure S28).

Based on these observations, and previous reports for the reaction of Co(I) complexes with NO_2^-, we therefore hypothesized an ECE mechanism that leads to the formation of a cobalt nitrosyl complex

$$[Co(CR)]^{2+} + e^- \rightleftarrows [Co(CR)]^+$$

$$[Co(CR)]^+ + NO_2^- + 2H^+ \rightarrow [Co(CR)(NO)]^{2+} + 2H_2O$$

$$[Co(CR)(NO)]^{2+} + e^- \rightarrow [Co(CR)(NO)]^+$$

Similar stoichiometric transformations have been observed in other cobalt complexes.[28,29] To test this hypothesis, we conducted a controlled potential electrolysis (CPE) experiment of $[Co(DIM)Br_2]^+$ in the presence of $NaNO_2$ at −0.99 V_{SCE}. The IR spectrum of the dark brown solid obtained following aerobic workup (Figure S29) reveals a strong band (ν_{NO} = 1642 cm^{-1}), consistent with that previously reported $[Co(CR)NO(Br)]^+$.[30]

Scanning to more negative potentials reveals a catalytic current for NO_2^- reduction, with an onset potential (−0.98 V_{SCE}) that coincides with the $Co^{I}(L/L^{\bullet-})$ couple (Figure 5a). The current is dependent on NO_2^- concentration, consistent with the electrocatalytic reduction of aqueous NO_2^- by $[Co(CR)Br_2]^+$. Product analysis following CPE at −1.46 V_{SCE} confirms electrocatalytic NO_2^- reduction, with 1 h electrolysis at the initial pH 6.40 providing high yields of ammonium (88% Faradaic efficiency)[31] (Figure 5b).

We conducted a number of experiments to test for catalyst homogeneity. Notably, the results of a "dip-and-stir" test[32] suggest that a catalytically active material is deposited on the electrode surface. X-ray photoelectron spectroscopy confirms the presence of cobalt in this material. The electrochemical signature of this material differs from that of $[Co(CR)Br_2]^+$, with the onset of electrocatalysis occurring at a more cathodic potential for the deposition (Figure S20). The CV of this material also differs from that of cobalt nanoparticles.[33] Together, this suggests that both homogeneous and heterogeneous species contribute to the electrocatalytic reduction of nitrite by $[Co(CR)Br_2]^+$.

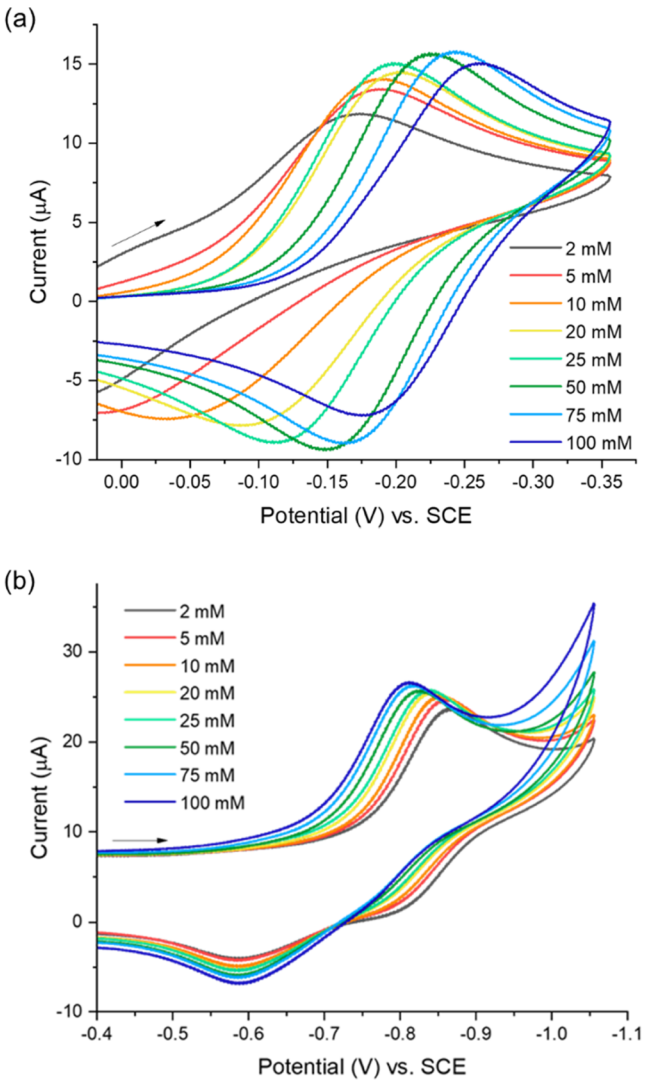

Figure 4. Cyclic voltammograms of (a) the $Co^{III/II}$ couple and (b) the $Co^{II/I}$ couple with 1 mM $[Co(CR)Br_2]^+$ in 0.1 M Na_2SO_4 with variable $NaNO_2$ concentration. Conditions: glassy carbon working electrode, Pt wire counter electrode, 100 mV s^{-1}.

https://doi.org/10.1021/acs.inorgchem.2c00199
Inorg. Chem. 2022, 61, 9034−9039

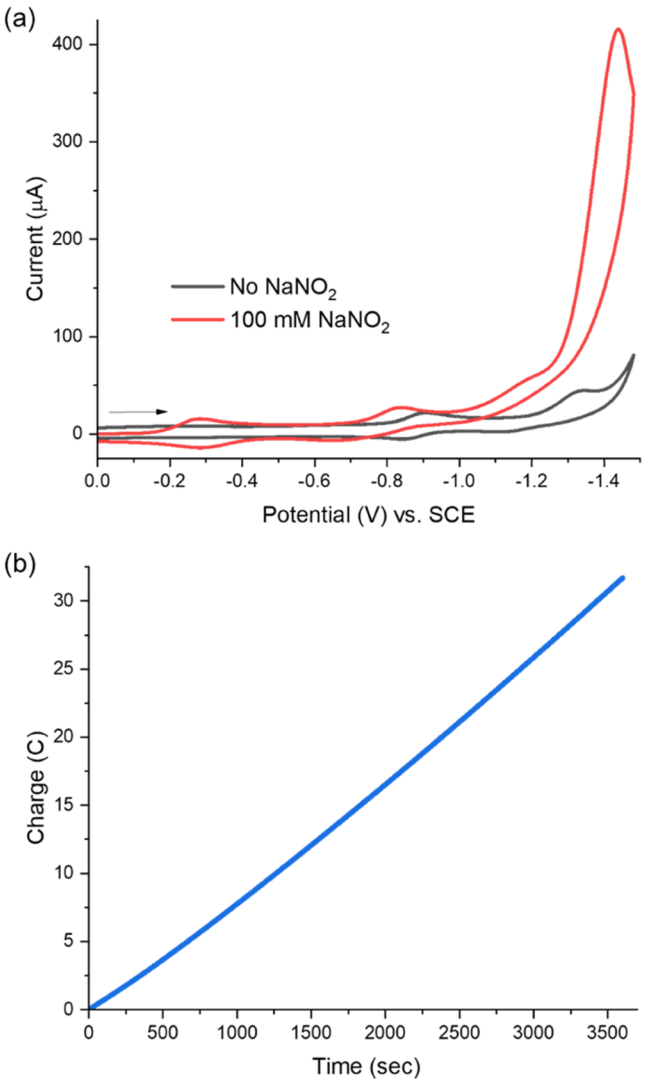

Figure 5. (a) Cyclic voltammograms of 1 mM $[Co(CR)Br_2]^+$ in 0.1 M Na_2SO_4 with varying concentrations of NO_2^-. Conditions: glassy carbon working electrode, Pt wire counter electrode, 100 mV s^{-1}. (b) Controlled-potential electrolysis at −1.46 V_{SCE} of 1 mM $[Co(CR)Br_2]^+$ with 100 mM $NaNO_2$ in 0.1 M KCl aqueous solution with a glassy carbon rod working electrode.

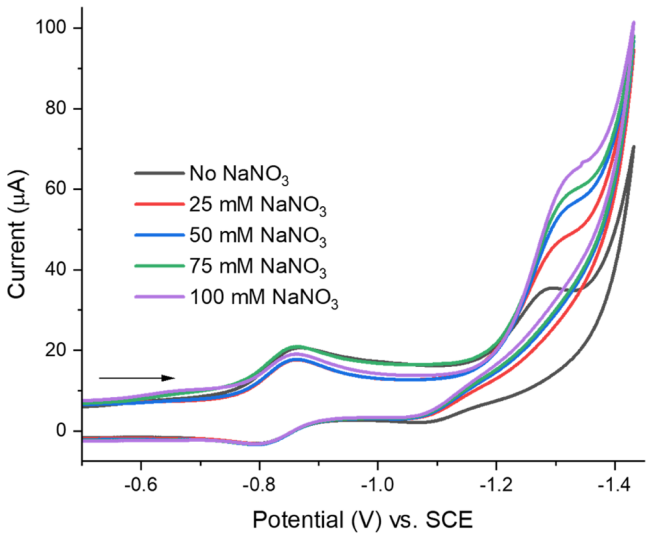

Figure 6. Cyclic voltammograms of 1 mM $[Co(CR)Br_2]^+$ with variable concentrations of $NaNO_3$ in 0.1 M Na_2SO_4. Conditions: glassy carbon working electrode, Pt wire counter electrode, 100 mV s^{-1}.

Electrocatalytic Nitrate Reduction. In contrast to NO_2^-, no changes in the $Co^{III/II}$ and $Co^{II/I}$ waves are observed for the CV of $[Co(CR)Br_2]^+$ in the presence of 25 mM NO_3^-. Nonetheless, a modest catalytic current is observed, with an onset potential (−1.18 V_{SCE}) that is also similar to the potential for the $Co^I(L/L^{\bullet-})$ process. As expected for electrocatalysis, the current increases with increasing NO_3^- concentration (Figure 6), although it is significantly lower than observed for NO_2^- reduction. This is similar to our previous observations with $[Co(DIM)Br_2]^+$.[13,14] Product analysis following controlled-potential electrolysis (CPE) at −1.36 V_{SCE} confirms electrocatalytic NO_3^- reduction (Figure S30); however, the catalytic efficiency is poorer than for the reduction of NO_2^-. Moderate quantities of ammonium (57% Faradaic efficiency)[31] and small quantities of NO_2^- (3% Faradaic efficiency)[34] are formed following 2 h CPE. No hydroxylamine is detected.[35]

It is important to note that NO_3^- is reduced to NO_2^- at the glassy carbon electrode even in the absence of $[Co(CR)Br_2]^+$ catalyst. For example, CPE for 2 h at an applied potential of −1.36 V_{SCE} provides NO_2^- with a 22% Faradaic efficiency.[36] Since this Faradaic efficiency decreases in the presence of $[Co(CR)Br_2]^+$, it is conceivable that NO_3^- is initially reduced to NO_2^- at the electrode surface, with the reduction to ammonium being catalyzed by $[Co(CR)Br_2]^+$. To test this hypothesis, we conducted additional electrochemical experiments using a mercury pool working electrode. Importantly, this electrode shows no current enhancement for the CV of NO_3^- in the absence of $[Co(CR)Br_2]^+$. In this case, NO_2^- is observed following 2 h of CPE at −1.54 V_{SCE} in the presence of $[Co(CR)Br_2]^+$ (Figure S32). Together, these experiments indicate that $[Co(CR)Br_2]^+$ is catalytically active for the reduction of both NO_3^- and NO_2^-.

CONCLUSIONS

We have shown that the macrocyclic complex $[Co(CR)Br_2]^+$ is an electrocatalyst for the reduction of aqueous NO_2^- and NO_3^-. These results provide support for the electrocatalyst design criteria delineated from our previous studies of $[Co(DIM)Br_2]^+$.[13,14] Specifically, $[Co(CR)Br_2]^+$ is based on a flexible macrocycle that also provides redox activity and an intramolecular proton shuttle.

Both nitrogen oxyanions are ultimately reduced to ammonium, although the reduction of NO_2^- occurs with much greater Faradaic efficiency. Interestingly, there is evidence for both homogeneous and heterogeneous electrocatalysis by $[Co(DIM)Br_2]^+$. In the case of NO_3^-, small quantities of free NO_2^- are also formed as an intermediate species. This contrasts with $[Co(DIM)Br_2]^+$, where there is no evidence for the intermediate formation of free NO_2^-.[14] It is important to note that NO_3^- can be reduced to NO_2^- at the glassy carbon electrode in the absence of catalyst. Although the Faradaic efficiency is poor, this reduction occurs at potentials similar to those for which the electrocatalyst is operative.

There are now multiple cobalt-based macrocyclic complexes for electrocatalytic NO_3^- reduction. Despite the favorable thermodynamics for NO_3^- reduction, it is notable that all of these electrocatalysts operate with a very large overpotential

https://doi.org/10.1021/acs.inorgchem.2c00199
Inorg. Chem. 2022, 61, 9034−9039

(>1 V). Mechanistically, this large overpotential can be attributed in part to the need for the N−O bond cleavage to occur by two-electron steps, as demonstrated for [Co(DIM)-Br_2]$^+$.[13] Nitrate reduction therefore requires the catalyst to be reduced from Co(III) to the formally Co(I) oxidation state. In the case of redox innocent ligands such as cyclam, the onset potential for electrocatalysis is therefore dictated by the potential required to access Co(I). While the ability of redox noninnocent ligands to store electrons makes access to the equivalent redox state in these complexes more accessible, relatively cathodic potentials are still required.[15] We anticipate that ligands that better stabilize the formally Co(I) state in aqueous solution will allow for nitrate reduction electrocatalysis with smaller overpotentials.

■ ASSOCIATED CONTENT

Supporting Information

The Supporting Information is available free of charge at https://pubs.acs.org/doi/10.1021/acs.inorgchem.2c00199.

Complete experimental details, including electrochemical and electrocatalysis experiments (PDF)

■ AUTHOR INFORMATION

Corresponding Author

Jeremy M. Smith − *Department of Chemistry, Indiana University, Bloomington, Indiana 47405, United States;* orcid.org/0000-0002-3206-4725; Email: smith962@indiana.edu

Authors

Sheyda Partovi − *Department of Chemistry, Indiana University, Bloomington, Indiana 47405, United States*

Ziqing Xiong − *Department of Chemistry, Indiana University, Bloomington, Indiana 47405, United States*

Krista M. Kulesa − *Department of Chemistry, Indiana University, Bloomington, Indiana 47405, United States;* orcid.org/0000-0003-4074-5464

Complete contact information is available at: https://pubs.acs.org/10.1021/acs.inorgchem.2c00199

Notes

The authors declare no competing financial interest.

■ ACKNOWLEDGMENTS

The authors gratefully acknowledge funding from the NSF (CHE-1900020). The authors thank Sarah E. Braley for helpful discussions and for running XPS. The authors would also like to thank Kaustav Chatterjee and Nayana Christudas Beena for GC-TCD sampling.

■ REFERENCES

(1) Galloway, J. N.; Leach, A. M.; Bleeker, A.; Erisman, J. W. A Chronology of Human Understanding of the Nitrogen Cycle. *Philos. Trans. R. Soc. Lond., B: Biol. Sci.* **2013**, *368*, No. 20130120.

(2) Matassa, S.; Batstone, D. J.; Hülsen, T.; Schnoor, J.; Verstraete, W. Can Direct Conversion of Used Nitrogen to New Feed and Protein Help Feed the World? *Environ. Sci. Technol.* **2015**, *49*, 5247−5254.

(3) Bollmann, A.; French, E.; Laanbroek, H. J. Isolation, Cultivation, and Characterization of Ammonia-Oxidizing Bacteria and Archaea Adapted to Low Ammonium Concentrations. In *Methods in Enzymology*, Klotz, M. G., Ed.; Academic Press, 2011; Vol. *486*, Chapter 3, pp 55−88.

(4) Selman, M.; Sugg, Z.; Greenhalgh, S.; Diaz, R. *Eutrophication and Hypoxia in Coastal Areas: A Global Assessment of the State of Knowledge*, WRI Policy Note, 2008.

(5) Stuhldreier, I.; Bastian, P.; Schönig, E.; Wild, C. Effects of simulated eutrophication and overfishing on algae and invertebrate settlement in a coral reef of Koh Phangan, Gulf of Thailand. *Mar. Pollut. Bull.* **2015**, *92*, 35−44.

(6) Camargo, J. A.; Alonso, Á. Ecological and toxicological effects of inorganic nitrogen pollution in aquatic ecosystems: A global assessment. *Environ. Int.* **2006**, *32*, 831−849.

(7) Rountree, E. S.; McCarthy, B. D.; Eisenhart, T. T.; Dempsey, J. L. Evaluation of Homogeneous Electrocatalysts by Cyclic Voltammetry. *Inorg. Chem.* **2014**, *53*, 9983−10002.

(8) Guldi, D.; Wasgestian, F.; Meyerstein, D. The Effect of N-Methylation on the Spectroscopical and Electrochemical Properties of 1,4,8,11-tetraazacyclotetradecane Chromium(III) Complexes. *Inorg. Chim. Acta* **1992**, *194*, 15−22.

(9) Braley, S. E.; Ashley, D. C.; Jakubikova, E.; Smith, J. M. Electrode-adsorption activates *trans*-[Cr(cyclam)Cl_2]$^+$ for electrocatalytic nitrate reduction. *Chem. Commun.* **2020**, *56*, 603−606.

(10) Cheng, S.-H.; Su, Y. O. Electrocatalysis of Nitric Oxide Reduction by Water-Soluble Cobalt Porphyrin. Spectral and Electrochemical Studies. *Inorg. Chem.* **1994**, *33*, 5847−5854.

(11) Stroka, J. R.; Kandemir, B.; Matson, E. M.; Bren, K. L. Electrocatalytic Multielectron Nitrite Reduction in Water by an Iron Complex. *ACS Catal.* **2020**, *10*, 13968−13972.

(12) Taniguchi, I.; Nakashima, N.; Matsushita, K.; Yasukouchi, K. Electrocatalytic reduction of nitrate and nitrite to hydroxylamine and ammonia using metal cyclams. *J. Electroanal. Chem. Interfacial Electrochem.* **1987**, *224*, 199−209.

(13) Xu, S.; Ashley, D. C.; Kwon, H.-Y.; Ware, G. R.; Chen, C.-H.; Losovyj, Y.; Gao, X.; Jakubikova, E.; Smith, J. M. A Flexible, Redox-Active Macrocycle Enables the Electrocatalytic Reduction of Nitrate to Ammonia by a Cobalt Complex. *Chem. Sci.* **2018**, *9*, 4950−4958.

(14) Xu, S.; Kwon, H.-Y.; Ashley, D. C.; Chen, C.-H.; Jakubikova, E.; Smith, J. M. Intramolecular Hydrogen Bonding Facilitates Electrocatalytic Reduction of Nitrite in Aqueous Solutions. *Inorg. Chem.* **2019**, *58*, 9443−9451.

(15) Kwon, H.-Y.; Braley, S. E.; Madriaga, J. P.; Smith, J. M.; Jakubikova, E. Electrocatalytic nitrate reduction with Co-based catalysts: comparison of DIM, TIM and cyclam ligands. *Dalton Trans.* **2021**, *50*, 12324−12331.

(16) Ochiai, E.-i.; Busch, D. H. Organic derivatives of a cobalt(III) macrocylic complex. *Chem. Commun.* **1968**, 905−906.

(17) Römelt, C.; Weyhermüller, T.; Wieghardt, K. Structural characteristics of redox-active pyridine-1,6-diimine complexes: Electronic structures and ligand oxidation levels. *Coord. Chem. Rev.* **2019**, *380*, 287−317.

(18) Mousavi, M.; Duhayon, C.; Bretosh, K.; Béreau, V.; Sutter, J.-P. Molybdenum(III) Thiocyanate- and Selenocyanate-Based One-Dimensional Heteronuclear Polymers: Coordination Affinity-Controlled Assemblage of Mixed Spin and Mixed Valence Derivatives with Ni(II) and Co(II/III). *Inorg. Chem.* **2020**, *59*, 7603−7613.

(19) Wyllie, G. R. A.; Munro, O. Q.; Schulz, C. E.; Robert Scheidt, W. Structural and physical characterization of (nitrato)iron(III) porphyrinates [Fe(por)(NO_3)] − Variable coordination of nitrate. *Polyhedron* **2007**, *26*, 4664−4672.

(20) Timmons, A. J.; Symes, M. D. Converting between the oxides of nitrogen using metal−ligand coordination complexes. *Chem. Soc. Rev.* **2015**, *44*, 6708−6722.

(21) Leung, C.-F.; Chen, Y.-Z.; Yu, H.-Q.; Yiu, S.-M.; Ko, C.-C.; Lau, T.-C. Electro- and photocatalytic hydrogen generation in acetonitrile and aqueous solutions by a cobalt macrocyclic Schiff-base complex. *Int. J. Hydrogen Energy* **2011**, *36*, 11640−11645.

(22) Moonshiram, D.; Gimbert-Suriñach, C.; Guda, A.; Picon, A.; Lehmann, C. S.; Zhang, X.; Doumy, G.; March, A. M.; Benet-Buchholz, J.; Soldatov, A.; Llobet, A.; Southworth, S. H. Tracking the Structural and Electronic Configurations of a Cobalt Proton

Reduction Catalyst in Water. *J. Am. Chem. Soc.* **2016**, *138*, 10586−10596.
(23) Varma, S.; Castillo, C. E.; Stoll, T.; Fortage, J.; Blackman, A. G.; Molton, F.; Deronzier, A.; Collomb, M.-N. Efficient photocatalytic hydrogen production in water using a cobalt(III) tetraaza-macrocyclic catalyst: electrochemical generation of the low-valent Co(I) species and its reactivity toward proton reduction. *Phys. Chem. Chem. Phys.* **2013**, *15*, 17544−17552.
(24) Lacy, D. C.; McCrory, C. C. L.; Peters, J. C. Studies of Cobalt-Mediated Electrocatalytic CO_2 Reduction Using a Redox-Active Ligand. *Inorg. Chem.* **2014**, *53*, 4980−4988.
(25) Zhang, M.; El-Roz, M.; Frei, H.; Mendoza-Cortes, J. L.; Head-Gordon, M.; Lacy, D. C.; Peters, J. C. Visible Light Sensitized CO_2 Activation by the Tetraaza $[Co^{II}N_4H(MeCN)]^{2+}$ Complex Investigated by FT-IR Spectroscopy and DFT Calculations. *J. Phys. Chem. C* **2015**, *119*, 4645−4654.
(26) Siu, J. C.; Sauer, G. S.; Saha, A.; Macey, R. L.; Fu, N.; Chauviré, T.; Lancaster, K. M.; Lin, S. Electrochemical Azidooxygenation of Alkenes Mediated by a TEMPO−N_3 Charge-Transfer Complex. *J. Am. Chem. Soc.* **2018**, *140*, 12511−12520.
(27) Savéant, J.-M. Coupling of Electrode Electron Transfers with Homogeneous Chemical Reactions. In *Elements of Molecular and Biomolecular Electrochemistry*, Wiley, 2006; pp 78−181.
(28) Cabelof, A. C.; Carta, V.; Chen, C.-H.; Caulton, K. G. Nitrogen oxyanion reduction by Co(II) augmented by a proton responsive ligand: recruiting multiple metals. *Dalton Trans.* **2020**, *49*, 7891−7896.
(29) Uyeda, C.; Peters, J. C. Selective Nitrite Reduction at Heterobimetallic CoMg Complexes. *J. Am. Chem. Soc.* **2013**, *135*, 12023−12031.
(30) Long, K. M.; Busch, D. H. Cobalt(III) Complexes of the Tetradentate Macrocycle 2, 12-Dimethyl-3, 7, 11, 17-Tetraazabicyclo(11.3.1)Heptadeca-1(17),2,11,13,15-Pentaene. *J. Coord. Chem.* **1974**, *4*, 113−123.
(31) Weatherburn, M. W. Phenol-hypochlorite reaction for determination of ammonia. *Anal. Chem.* **1967**, *39*, 971−974.
(32) Alvarez-Hernandez, J. L.; Han, J. W.; Sopchak, A. E.; Guo, Y.; Bren, K. L. Linear Free Energy Relationships in Hydrogen Evolution Catalysis by a Cobalt Tripeptide in Water. *ACS Energy Lett.* **2021**, *6*, 2256−2261.
(33) Ghosh, M.; Ibrar, M.; Smith, J. M. Electrocatalytic reduction of nitrate by in situ generated cobalt nanoparticles. *Chem. Commun.* **2022**, *58*, 4783−4786.
(34) Rider, B. F.; Mellon, M. G. Colorimetric Determination of Nitrites. *Ind. Eng. Chem., Anal. Ed.* **1946**, *18*, 96−99.
(35) Frear, D. S.; Burrell, R. C. Spectrophotometric Method for Determining Hydroxylamine Reductase Activity in Higher Plants. *Anal. Chem.* **1955**, *27*, 1664−1665.
(36) When the potential is held at −1.28 V vs SCE the Faradaic efficiency for nitrate reduction to nitrite is 11%.

https://doi.org/10.1021/acs.inorgchem.2c00199
Inorg. Chem. 2022, 61, 9034−9039